JOURNAL OF SOLID STATE CHEMISTRY 110, 156–161 (1994)

Synthesis of the New Quaternary Sulfides $K_2Y_4Sn_2S_{11}$ and Ba*Ln*AgS_3 (*Ln* = Er, Y, Gd) and the Structures of $K_2Y_4Sn_2S_{11}$ and $BaErAgS_3$

Ping Wu and James A. Ibers

Department of Chemistry, Northwestern University, Evanston, Illinois 60208-3113

Received June 7, 1993; in revised form August 16, 1993; accepted August 17, 1993

Several new quaternary sulfides, $K_2Y_4Sn_2S_{11}$ and Ba*Ln*AgS_3 (*Ln* = Er, Y, Gd), have been synthesized by the reaction of the constituent binary chalcogenides and elements at 1000°C. The crystal structures of $K_2Y_4Sn_2S_{11}$ and $BaErAgS_3$ have been determined by single-crystal X-ray diffraction techniques. Crystal data: $K_2Y_4Sn_2S_{11}$—space group D_{4h}^8 – $P4/ncc$, M = 1023.88, Z = 4, a = 8.587(1), c = 27.892(4) Å (T = 115 K), V = 2056.7(4) Å^3, $R_w(F^2)$ = 0.093 for 1965 observations and 48 variables, $R(F)$ = 0.034 for 1319 observations having $F_o^2 > 2\sigma(F_o^2)$; $BaErAgS_3$—space group C_{2h}^3 – $C2/m$, M = 508.65, Z = 4, a = 17.340(4), b = 4.014(1), c = 8.509(2) Å, β = 103.23(3)°, (T = 115 K), V = 576.5(2) Å^3, $R_w(F^2)$ = 0.049 for 1404 observations and 48 variables, $R(F)$ = 0.018 for 1299 observations having $F_o^2 > 2\sigma(F_o^2)$. In both structures the rare-earth atoms have octahedral coordination and the octahedra form slabs through edge- and corner-sharing. These slabs are separated by K^+ or Ba^{2+} cations, and are crosslinked into three-dimensional frameworks by Sn_2S_6 units as edge-sharing SnS_4 tetrahedral pairs in $K_2Y_4Sn_2S_{11}$, and by Ag_2S_9 units as corner-sharing trigonal-bipyramidal AgS_5 pairs in $BaErAgS_3$. From their powder diffraction patterns, $BaYAgS_3$ and $BaGdAgS_3$ appear to be isostructural with $BaErAgS_3$.

INTRODUCTION

Recently, several new series of quaternary chalcogenides that contain a rare-earth metal, an alkali- or alkaline-earth metal, and a main-group or transition metal have been synthesized (1–5). Although cation disorder occurs in some compounds that contain one of the smaller rare-earth elements and a small s-block metal element (e.g., $CaYbInS_3$ (5)), most of these structures have crystallographically distinct sites for the three different types of metal atoms, and there is no disorder. This results in a wide range of structural features that can be described by the packing of metal–chalcogen polyhedra. Furthermore, the structural features may be modified through the substitution of different rare-earth elements (1). Here we describe the synthesis and structures of two new types of quaternary sulfides, $K_2Y_4Sn_2S_{11}$ and Ba*Ln*AgS_3 (*Ln* = Er, Y, Gd), and the structural characterization of $K_2Y_4Sn_2S_{11}$ and $BaErAgS_3$.

EXPERIMENTAL

Syntheses. $K_2Y_4Sn_2S_{11}$ was prepared by the reaction of K_2S_5 (prepared from elemental K (AESAR, 99%) and S (Alfa, 99.9995%)) with Y_2S_3 (prepared from elemental Y (Johnson Matthey, 99.9%) and S) and Sn powder (Johnson Matthey, 99.999%) in a quartz tube that was evacuated to 10^{-5} Torr. The reaction that produced the crystal for the structure determination had a molar ratio of 1 : 1 : 2 for the starting materials. The mixture was heated gradually to 500°C where it was kept for 24 hr before being successively brought to 700°C for 24 hr and to 1000°C for 150 hr. The tube was then cooled at a rate of 4°C/hr to 300°C and then the furnace was shut off. Small light-yellow plates had grown in the tube, usually in a mixture with other binary and ternary sulfides. EDAX analysis with the microprobe of a Hitachi S-570 scanning electron microscope confirmed the presence of all four elements in the crystals, and an elemental ratio of approximately 1 : 2 : 1 was found for K : Y : Sn. The exact stoichiometry was determined from the single-crystal structure determination.

The compounds Ba*Ln*AgS_3 (*Ln* = Er, Y, Gd) were prepared by the reactions of elemental Ag (AESAR, 99.999%) and S with the binary sulfides BaS (AESAR, 99.9%) and Ln_2S_3 (prepared by high-temperature reactions of rare-earth metals (all from Johnson Matthey, 99.9%) with S). After a preliminary study, an elemental ratio of 1 : 1 : 1 : 3 for Ba : *Ln* : Ag : S was used. To grow single crystals of $BaErAgS_3$, the same heating sequence described above was used. Orange-red crystals of $BaErAgS_3$ had grown in the tubes. Semiquantitative EDAX analysis confirmed the presence of all four elements in a ratio of approximately 1 : 1 : 1 : 3. Bulk samples of these three compounds were prepared by reactions of stoichiometric amounts of starting materials at 850°C for 6 days with an intermittent grinding.

Crystallographic study of $K_2Y_4Sn_2S_{11}$. A preliminary unit cell and space group were determined at room temperature by Weissenberg photography. A platelike crystal of approximate dimensions 0.04 by 0.17 by 0.21 mm was

0022-4596/94 $6.00

TABLE 1
Crystal Data and Experimental Details for $K_2Y_4Sn_2S_{11}$ and $BaErAgS_3$

Compound	$K_2Y_4Sn_2S_{11}$	$BaErAgS_3$
Formula weight	1023.88	508.65
Space group	D_{4h}^8–$P4/ncc$	C_{2h}^3–$C2/m$
a (Å)	8.587(1)	17.340(4)
b (Å)	8.587	4.014(1)
c (Å)	27.892(4)	8.509(2)
β (deg.)	90	103.23(3)
V (Å^3)	2056.7(4)	576.5(2)
Z	4	4
T of data collection (K)	115[a]	115[b]
Crystal vol. (mm^3)	1.2×10^{-3}	1.4×10^{-4}
Crystal shape	Plate, bounded by {110}, {001} and (130)	Needle, bounded by {100}, {010}, {001}, {20$\bar{1}$}
Radiation	Graphite monochromated Mo$K\alpha$ ($\lambda(K\alpha_1)$ = 0.7093 Å)	Graphite monochromated Mo$K\alpha$ ($\lambda(K\alpha_1)$ = 0.7093 Å)
Linear abs. coeff. (cm^{-1})	150.5	254.7
Transmission factors[c]	0.149–0.526	0.395–0.563
Detector aperture (mm)	Horizontal, 4.3; vertical, 4.3; 32 cm from crystal	Horizontal, 4.0; vertical, 2.0; 20 cm from crystal
Take-off angle (deg.)	2.5	3.0
Scan speed (deg. min^{-1})	$2.5° \le 2\theta \le 50°$, 3.0 in 2θ; $50° \le 2\theta \le 66°$, 2.0 in 2θ	2.0[d] in 2θ
Scan type	θ–2θ	ω–2θ
Scan range (deg.)	0.7° below $K\alpha_1$ to 0.9° above $K\alpha_2$	0.9° below $K\alpha_1$ to 0.9° above $K\alpha_2$
$\lambda^{-1} \sin\theta$, limits (Å^{-1})	0.0308–0.7679	0.0492–0.8087
	$2.5° \le 2\theta(MoK\alpha_1) \le 66°$	$4° \le 2\theta(MoK\alpha_1) \le 70°$
Background counts	$2.5° \le 2\theta \le 50°$, 6.0 sec; and $50° \le 2\theta \le 66°$, 9.0 sec at each end of the scan	4.8 sec at each end of the scan
Data collected	$2.5° \le 2\theta(MoK\alpha_1) \le 35°$, $\pm h \pm k \pm l$; $35° \le 2\theta(MoK\alpha_1) \le 66°$, $\pm h \pm k + l$	$\pm h \pm k \pm l$
No. of unique data including $F_o^2 < 0$	1965	1404
No. of unique data with $F_o^2 > 2\sigma(F_o^2)$	1319	1299
No. of variables	48	40
$R_w(F^2)$[e]	0.093	0.049
R [on F for $F_o^2 > 2\sigma(F_o^2)$]	0.034	0.018
Error in observation of unit weight	1.14	0.89

[a] The low-temperature system for the Picker diffractometer is based on a design by Huffman (17).
[b] The low-temperature system for the Nonius CAD4 diffractometer is from a design by Professor J. J. Bonnet and S. Askenazy and is commercially available from Soterem, Z. T. de Vic, 31320 Castanet-Tolosan, France.
[c] The analytical method was used for the absorption correction (18).
[d] Reflections with $\sigma(I)/I > 0.33$ were rescanned up to a maximum of 50 sec.
[e] $w^{-1} = \sigma^2(F_o^2) + (0.04 \times F_o^2)^2$ for $F_o^2 \ge 0$ and $w^{-1} = \sigma^2(F_o^2)$ for $F_o^2 < 0$.

selected for data collection. Intensity data were collected by the θ–2θ scan technique on a Picker diffractometer. The lattice constants were determined from a least-squares analysis of the setting angles of 38 reflections in the range $35° < 2\theta\,(MoK\alpha_1) < 40°$ that had been automatically centered at 115 K. The refined cell constants and additional relevant crystal data are given in Table 1. Six standard reflections measured every 100 reflections throughout data collection decayed by 10% on average by the end of the data collection.

The initial data processing was carried out on a Stardent computer with programs and methods standard in this laboratory. The space group was determined to be $P4/ncc$ from the systematic absences. Data were corrected for decay and absorption and then averaged. The residual for averaging is 10.4% for all the data and 6.3% for the data with $F_o^2 > 2\sigma(F_o^2)$. Two heavy-atom sites were found with the use of the automatic Patterson interpretation routine in the program SHELXS (6). The rest of the atoms were located from difference electron-density maps after iterations of isotropic least-squares refinement. The resultant R index on F was 0.045 for those reflections having $F_o^2 > 2\sigma(F_o^2)$. The final anisotropic refinement on F_o^2 employed all reflections except for two with very negative

TABLE 2
Atomic Coordinates and Equivalent Isotropic Displacement Parameters ($Å^2 \times 10^3$)[a] for $K_2Y_4Sn_2S_{11}$ and $BaErAgS_3$

Compound	x	y	z	U_{eq}
		$K_2Y_4Sn_2S_{11}$		
Sn	$\frac{3}{4}$	$\frac{1}{4}$	0.1908(1)	7(1)
Y	0.1439(1)	0.5516(1)	0.0549(1)	6(1)
K(1)	$\frac{1}{4}$	$\frac{1}{4}$	0.1966(1)	16(1)
K(2)	$\frac{1}{4}$	$\frac{1}{4}$	0.3724(1)	18(1)
S(1)	0.0888(2)	0.5733(2)	0.1489(1)	10(1)
S(2)	0.6460(1)	0.0574(2)	0.0451(1)	7(1)
S(3)	0.3977(1)	0.6023(1)	$\frac{1}{4}$	11(1)
S(4)	$\frac{1}{4}$	$\frac{1}{4}$	0.0588(1)	8(1)
		$BaErAgS_3$		
Er	0.1638(1)	0	0.0805(1)	4(1)
Ba	0.1360(1)	0	0.5685(1)	5(1)
Ag	0.5138(1)	0	0.2089(1)	20(1)
S(1)	0.3263(1)	0	0.1317(1)	5(1)
S(2)	0.6764(1)	0	0.3014(1)	5(1)
S(3)	0	$\frac{1}{2}$	$\frac{1}{2}$	6(1)
S(4)	0	0	0	9(1)

[a] $U_{eq} = \frac{1}{3} \Sigma_i \Sigma_j U_{ij} a_i^* a_j^* \mathbf{a}_i \cdot \mathbf{a}_j$.

F_o^2 (7). Values of the resultant R indices are 0.093 for $R_w(F^2)$ (all data) and 0.034 for $R(F)$ ($F_o^2 > 2\sigma(F_o^2)$). The highest residual electron density peak has a height of about 0.6% that of a Sn atom. The program package SHELXTL PC (6) was used for the ensuing molecular graphics generation.

Crystallographic study of $BaErAgS_3$. A preliminary unit cell and space group were determined at room temperature by Weissenberg photography. A needlelike crystal of approximate dimensions 0.03 by 0.04 by 0.16 mm was selected for data collection. The lattice constants were determined from a least-squares analysis of the setting angles of 25 reflections in the range $30° < 2\theta$ ($MoK\alpha_1$) $< 40°$ that had been automatically centered at 115 K on a CAD4 diffractometer. The refined cell constants and additional relevant crystal data are given in Table 1. Intensity data were collected by the ω–2θ scan technique. Six standard reflections measured every 3 hr throughout data collection showed no significant variations in intensity. From the systematic absences, the space groups $C2/m$, $C2$, or Cm were possible. Data were corrected for absorption and then averaged. That the residual for averaging the reflections in Laue group $2/m$ is 3.1% is a strong indication that the material crystallizes in the centrosymmetric space group $C2/m$. With the direct methods program SHELXS (6), a solution was found in this space group. This solution refined isotropically to an R index on F of 0.058. The final anisotropic refinement on F_o^2 employed all of the unique data (7). Values of the resultant R indices are 0.049 for $R_w(F^2)$ (all data) and 0.018 for $R(F)$ ($F_o^2 > 2\sigma(F_o^2)$). The highest residual electron-density peak has a height less than 0.4% that of an Er atom.

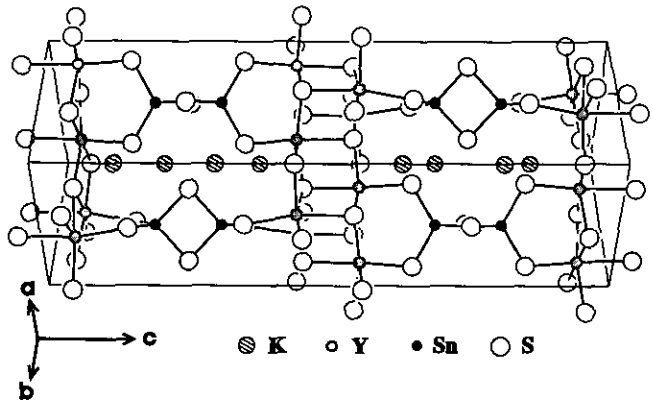

FIG. 1. Perspective view down [110] of the $K_2Y_4Sn_2S_{11}$ structure. The unit cell is outlined.

In the both systems, no unusual trends were found in the goodness of fit as a function of F_o or scattering angle. Final values of the atomic parameters and equivalent isotropic displacement parameters appear in Table 2. Final anisotropic displacement parameters and structure amplitudes are given in Tables 3,[1] 4,[1] and 5.[1]

X-ray powder diffraction measurements. For phase identification, X-ray powder diffraction patterns of bulk samples were taken on a Philips powder diffractometer.

RESULTS AND DISCUSSION

Selected distances and angles for $K_2Y_4Sn_2S_{11}$ are given in Table 6 and a more comprehensive tabulation is in Table 7.[1] Figure 1 provides a perspective view of the structure. Sn atoms are coordinated by four S atoms at the corners of a tetrahedron, and Y atoms are coordinated by six S atoms at the corners of an octahedron. These octahedra are connected into a layer along the a–b plane by edge-sharing (Fig. 2). A pair of such layers forms a slab in the structure, and these slabs are crosslinked by Sn_2S_6 units (pairs of edge-sharing SnS_4 tetrahedra). The slabs resemble the NaCl structure, with two inner layers with both cations and anions and two outer layers with only anions. The S atoms in the inner layers are coordi-

[1] See NAPS document No. 05062 for 22 pages of supplementary material. Order from ASIS/NAPS, Microfiche Publications, P.O. Box 3513, Grand Central Station, New York, NY 10163. Remit in advance $4.00 for microfiche copy or $8.35 for photocopy. All orders must be prepaid. Institutions and organizations may order by purchase order. However, there is a billing and handling charge for this service of $15. Foreign orders add $4.50 for postage and handling, for the first 20 pages, and $1.00 for additional 10 pages of material, $1.50 for postage of any microfiche orders.

TABLE 6
Selected Bond Lengths (Å) and Angles (deg) for $K_2Y_4Sn_2S_{11}$

Sn–S(1)#1	2.363(1)
Sn–S(1)#2	2.363(1)
Sn–S(3)#1	2.438(1)
Sn–S(3)#2	2.438(1)
Y–S(1)	2.670(1)
Y–S(2)#3	2.674(1)
Y–S(2)#4	2.703(1)
Y–S(2)#5	2.715(1)
Y–S(4)	2.747(1)
Y–S(2)#6	2.792(1)
K(1)–S(1)#2	3.375(2)
K(1)–S(1)	3.375(2)
K(1)–S(1)#4	3.375(2)
K(1)–S(1)#3	3.375(2)
K(1)–S(3)#2	3.603(1)
K(1)–S(3)#4	3.603(1)
K(1)–S(3)	3.603(1)
K(1)–S(3)#3	3.603(1)
K(2)–S(1)#7	3.335(2)
K(2)–S(1)#8	3.335(2)
K(2)–S(1)#9	3.335(2)
K(2)–S(1)#10	3.335(2)
K(2)–S(2)#11	3.614(2)
K(2)–S(2)#12	3.614(2)
K(2)–S(2)#13	3.614(2)
K(2)–S(2)#14	3.614(2)
S(1)#1–Sn–S(1)#2	120.73(7)
S(1)#1–Sn–S(3)#1	107.79(4)
S(1)#2–Sn–S(3)#1	111.36(4)
S(1)#1–Sn–S(3)#2	111.36(4)
S(1)#2–Sn–S(3)#2	107.79(4)
S(3)#1–Sn–S(3)#2	94.74(6)
S(1)–Y–S(2)#3	87.71(4)
S(1)–Y–S(2)#4	104.27(4)
S(2)#3–Y–S(2)#4	167.92(5)
S(1)–Y–S(2)#5	89.06(4)
S(2)#3–Y–S(2)#5	94.01(5)
S(2)#4–Y–S(2)#5	87.85(4)
S(1)–Y–S(4)	94.96(6)
S(2)#3–Y–S(4)	89.00(3)
S(2)#4–Y–S(4)	88.40(3)
S(2)#5–Y–S(4)	175.07(5)
S(1)–Y–S(2)#6	168.93(5)
S(2)#3–Y–S(2)#6	84.83(4)
S(2)#4–Y–S(2)#6	83.54(4)
S(2)#5–Y–S(2)#6	83.32(4)
S(4)–Y–S(2)#6	93.08(6)

Note. Symmetry transformations used to generate equivalent atoms: #1, $-y + 3/2, x, z$; #2, $y, -x + 1/2, z$; #3, $-x + 1/2, -y + 1/2, z$; #4, $-y + 1/2, x, z$; #5, $y, -x + 3/2, z$; #6, $x - 1/2, y + 1/2, -z$; #7, $y - 1/2, x + 1/2, -z + 1/2$; #8, $x + 1/2, -y + 1, -z + 1/2$; #9, $-y + 1, -x, -z + 1/2$; #10, $-x, y - 1/2, -z + 1/2$; #11, $-y, -x + 1, -z + 1/2$; #12, $-x + 1, y + 1/2, -z + 1/2$; #13, $x - 1/2, -y, -z + 1/2$; #14, $y + 1/2, x - 1/2, -z + 1/2$.

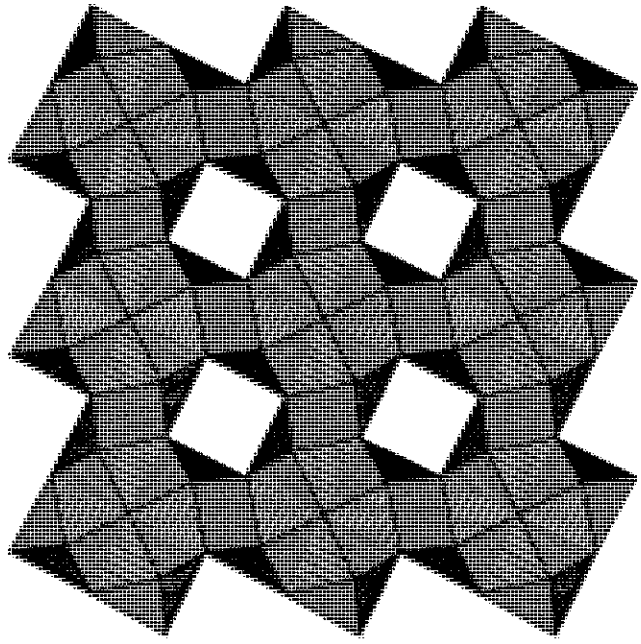

FIG. 2. A polyhedral representation of a layer of the Y–S octahedra in the $K_2Y_4Sn_2S_{11}$ structure.

nated by only three Y atoms in the same layer plus a fourth one in the adjacent layer; hence, one-fifth of the cation sites are vacant (as shown in Fig. 2). The edge-sharing tetrahedral pairs between the slabs resemble the building unit of the SiS_2 structure type (8). In the structure of $Na_4Sn_2S_6 \cdot 14H_2O$ (9), pairs of edge-sharing tetrahedra are isolated as $Sn_2S_6^{4-}$ anions by Na^+ cations. In the $BaHgSnS_4$ (10) and $BaCdSnS_4$ (11) structures, the tetrahedral pairs share corners to form three-dimensional frameworks. In the present structure, the adjacent pairs are oriented perpendicular to each other (Fig. 1), and the voids between the tetrahedral pairs are filled by K^+ cations. Both K^+ sites are coordinated by eight S atoms in a square-antiprismatic arrangement. As shown in Fig. I, the K^+ cations can also be viewed as occupying the channels along the [110] and [1$\bar{1}$0] directions.

Both the SnS_4 tetrahedra and the YS_6 octahedra are distorted in this structure, with the S–Sn–S bond angles ranging from 94.74(6) to 120.73(7)° and the cis S–Y–S angles ranging from 83.32(4) to 104.27(4)°. The Y–S bond lengths vary from 2.670(1) to 2.792(2) Å, and the Sn–S bond lengths vary from 2.363(1) to 2.438(1) Å. These values are comparable to those found in the literature. For example, Y–S bond lengths range from 2.69 to 2.92 Å in $YScS_3$ (12) and from 2.733(3) to 2.878(4) Å in CaY_2S_4 (13). In both compounds, Y is octahedrally coordinated. Sn–S bond lengths range from 2.325(2) to 2.452(2) Å in $Na_4Sn_2S_6 \cdot 14H_2O$ (9) and from 2.35 to 2.48 Å in $BaCdSnS_4$ (11).

Selected distances and angles for $BaErAgS_3$ are given

TABLE 8
Selected Bond Lengths (Å) and Angles (deg) for $BaErAgS_3$

Er–S(2)#1	2.725(1)
Er–S(2)#2	2.725(1)
Er–S(1)#3	2.731(1)
Er–S(1)#4	2.731(1)
Er–S(1)	2.752(1)
Er–S(4)	2.764(1)
Ba–S(3)#5	3.050(1)
Ba–S(3)	3.050(1)
Ba–S(2)#6	3.187(1)
Ba–S(1)#7	3.194(1)
Ba–S(1)#8	3.194(1)
Ba–S(2)#2	3.227(1)
Ba–S(2)#1	3.227(1)
Ag–S(3)#9	2.543(1)
Ag–S(4)#9	2.655(1)
Ag–S(4)#10	2.655(1)
Ag–S(2)	2.748(1)
Ag–S(1)	3.167(1)
S(2)#1–Er–S(2)#2	94.91(4)
S(2)#1–Er–S(1)#3	171.99(3)
S(2)#2–Er–S(1)#3	84.69(3)
S(2)#1–Er–S(1)#4	84.69(3)
S(2)#2–Er–S(1)#4	171.99(3)
S(1)#3–Er–S(1)#4	94.58(4)
S(2)#1–Er–S(1)	88.46(3)
S(2)#2–Er–S(1)	88.46(3)
S(1)#3–Er–S(1)	83.53(3)
S(1)#4–Er–S(1)	83.53(3)
S(2)#1–Er–S(4)	94.98(3)
S(2)#2–Er–S(4)	94.98(3)
S(1)#3–Er–S(4)	93.03(3)
S(1)#4–Er–S(4)	93.03(3)
S(1)–Er–S(4)	174.90(2)
S(3)#9–Ag–S(4)#9	129.64(1)
S(3)#9–Ag–S(4)#10	129.64(1)
S(4)#9–Ag–S(4)#10	98.21(2)
S(3)#9–Ag–S(2)	92.30(4)
S(4)#9–Ag–S(2)	96.97(3)
S(4)#10–Ag–S(2)	96.97(3)
S(3)#9–Ag–S(1)	83.16(4)
S(4)#9–Ag–S(1)	85.99(3)
S(4)#10–Ag–S(1)	85.99(3)
S(2)–Ag–S(1)	175.45(3)

Note. Symmetry transformations used to generate equivalent atoms: #1, $x - 1/2, y + 1/2, z$; #2, $x - 1/2, y - 1/2, z$; #3, $-x + 1/2, -y - 1/2, -z$; #4, $-x + 1/2, -y + 1/2, -z$; #5, $x, y - 1, z$; #6, $-x + 1, -y, -z + 1$; #7, $-x + 1/2, -y + 1/2, -z + 1$; #8, $-x + 1/2, -y - 1/2, -z + 1$; #9, $x + 1-2, y - 1/2, z$; #10, $x + 1/2, y + 1/2, z$.

in Table 8 and a more comprehensive tabulation is in Table 9.[1] Figure 3 shows the local coordination environment of the Er and Ag atoms with the labeling scheme for the S atoms. The Er atoms are coordinated by six S atoms at

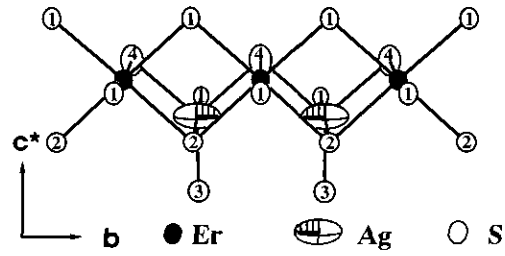

FIG. 3. Coordination geometry around the Er and Ag atoms in the $BaErAgS_3$ structure with the labeling scheme. The thermal ellipsoids are shown at 99.9% probability level.

the corners of an octahedron. The Er–S bond lengths range from 2.725(1) to 2.764(2) Å and compare well with those in the literature. For example, the Er–S bond lengths vary from 2.677(1) to 2.735(2) Å in $BaErCuS_3$ (1), and from 2.60(2) to 2.75(2) Å in $CrEr_2S_4$ (14). In both compounds, Er is octahedrally coordinated. Four of the shorter Ag–S bonds have lengths ranging from 2.543(1) to 2.748(1) Å. These values are close to the Ag–S bond lengths in the AgS_4 tetrahedra in $AgGaS_2$ (2.556(1) Å) (15) and in $Ba_2LaAg_5S_6$ (from 2.563(3) to 2.854(3) Å) (3). However, the AgS_4 tetrahedron in the present structure is highly distorted, with S–Ag–S angles ranging from 92.30(4) to 129.64(1)°. The coordination environment of the Ag atom can be better described as trigonal bipyramidal with a fifth S atom (S(1) in Fig. 3) included in the coordination sphere at a distance of 3.167(1) Å. This trigonal bipyramid is distorted because the Ag atom is shifted towards atom S(2). In addition to the unusual coordination about the Ag atom, its displacement ellipsoid is far from spherical, the displacement parameters being 0.020(1), 0.033(1), and 0.009(1) Å^2 for U_{11}, U_{22}, and U_{33}, respectively (Table 3[1] and Fig. 3).[2]

In this $BaErAgS_3$ structure, the ErS_6 octahedra share edges in a zigzag manner and form a double-chain along the b axis. These chains of octahedra then share corners to form $^2_\infty[Er_2S_5^{4-}]$ layers that are connected through pairs of corner-sharing Ag–S trigonal bipyramids (Ag_2S_9 units). Figure 4 is a polyhedral representation of such a layer and Fig. 5 provides a perspective view of the complete structure. It is a three-dimensional framework of ErS_6 octahedra and AgS_5 trigonal bipyramids. There are channels inside the framework that extend along the b axis. Ba^{2+} ions are accommodated in the monocapped trigonal prismatic sites inside the channels. The same kind of

[2] While it is inadvisable to give too much credence to vibrational ellipsoids in highly absorbing crystals, the possibility that this nonsphericity results from nonstoichiometry or from the presence of impurities was explored and discounted. A refinement of the data in which the occupancy of the Ag atom was an additional variable led to its occupancy being 0.992(2). EDAX analysis of the crystal used in the structure determination confirms the presence of only Ba, Er, Ag, and S.

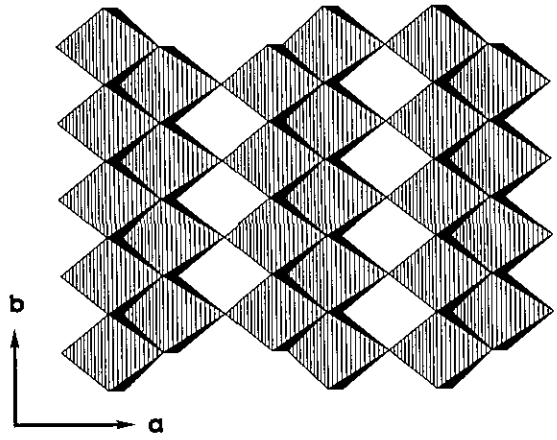

FIG. 4. A view along the c^* axis of a polyhedral representation of an $^2_\infty[Er_2S_5^{4-}]$ octahedral layer in the $BaErAgS_3$ structure.

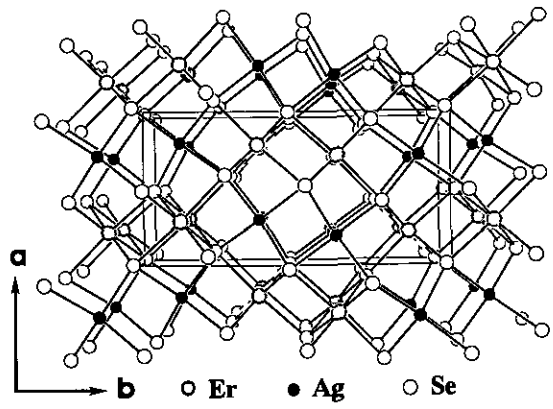

FIG. 6. View along the c axis of the $ErAgSe_2$ structure.

Er–chalcogen octahedral layers are found in $ErAgSe_2$ (Fig. 6) (16), where two sets of such layers intersect and form a three-dimensional structure. A comparison of Figs. 5 and 6 shows that the insertion of Ba^{2+} into the structure effectively separates the layers and results in a structure framework that is only linked through Ag_2S_9 units.

A comparison of Figs. 2 ($K_2Y_4Sn_2S_{11}$) and 4 ($BaErAgS_3$) reveals how the packing in these two structure types is related. In both structures there are double chains of edge-sharing LnS_4 octahedra. These chains can form layers either through further edge-sharing, as in $K_2Y_4Sn_2S_{11}$, or through corner-sharing, as in $BaErAgS_3$. In both, the layers are separated by cations and the connection is made through a pair of coordination polyhedra around the third metal element.

X-ray powder diffraction patterns obtained from polycrystalline samples of $BaYAgS_3$ and $BaGdAgS_3$ agree well with those calculated from the $BaErAgS_3$ structure. Thus, these three materials are probably isostructural.

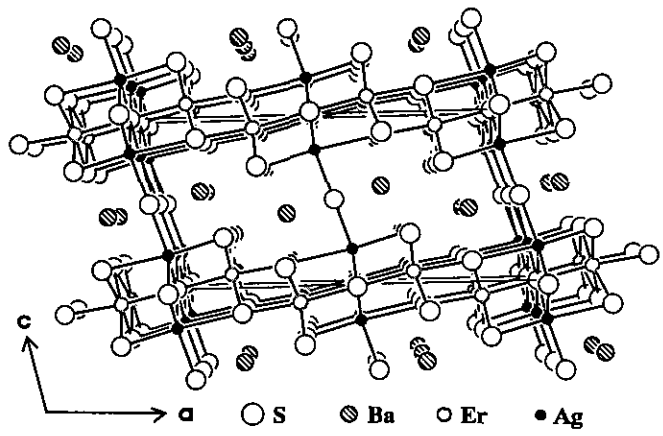

FIG. 5. View along the b axis of the $BaErAgS_3$ structure.

ACKNOWLEDGMENTS

Use was made of the X-ray and scanning electron microscope facilities supported by the National Science Foundation through the Northwestern University Materials Research Center, Grant DMR91-20521. This research was supported by the National Science Foundation through Grant DMR91-14934.

REFERENCES

1. P. Wu, A. E. Christuk, and J. A. Ibers, *J. Solid State Chem.*, in press.
2. A. E. Christuk, P. Wu, and J. A. Ibers, *J. Solid State Chem.*, in press.
3. P. Wu and J. A. Ibers, *Z. Kristallogr.* **208,** 35 (1993).
4. P. Wu and J. A. Ibers, *J. Solid State Chem.* **107,** 347 (1993).
5. J. D. Carpenter and S.-J. Hwu, *Chem. Mater.* **4,** 1368 (1992).
6. G. M. Sheldrick, SHELXTL PC Version 4.1, An Integrated System for Solving, Refining, and Displaying Crystal Structures from Diffraction Data. Siemens Analytical X-Ray Instruments, Inc., Madison, WI.
7. G. M. Sheldrick, SHELXL-92 Unix Beta-Test Version.
8. J. Peters and B. Krebs, *Acta Crystallogr., Sect. B: Struct. Crystallogr. Cryst. Chem.* **38,** 1270 (1982).
9. B. Krebs, S. Pohl, and W. Schiwy, *Z. Anorg. Allg. Chem.* **393,** 241 (1972).
10. C. L. Teske, *Z. Naturforsch., B: Anorg. Chem., Org. Chem.* **35,** 7 (1980).
11. C. L. Teske, *Z. Anorg. Allg. Chem.* **460,** 163 (1980).
12. N. Rodier and P. Laruelle, *C. R. Séances Acad. Sci., Ser. C* **270,** 2127 (1970).
13. A. Tomas, M. Guittard, and J. Flahaut, *Acta Crystallogr., Sect. B: Struct. Crystallogr. Cryst. Chem.* **42,** 364 (1986).
14. S. Jaulmes, *Acta Crystallogr., Sect. B: Struct. Crystallogr. Cryst. Chem.* **30,** 2283 (1974).
15. S. C. Abrahams and J. L. Bernstein, *J. Chem. Phys.* **59,** 1625 (1973).
16. M. Julien-Pouzol and P. Laruelle, *Acta Crystallogr., Sect. B: Struct. Crystallogr. Cryst. Chem.* **33,** 1510 (1977).
17. J. C. Huffman, Ph.D. thesis, Indiana University, 1974.
18. J. de Meulenaer and H. Tompa, *Acta Crystallogr.* **19,** 1014 (1965).